Electronic Supplementary Material (ESI) for Nanoscale.

Supporting Information

Designed synthesis of MO_x (M = Zn, Fe, Sn, Ni, Mn, Co, Ce, Mg, Ag), Pt, Au nanoparticles supported on hierarchical CuO hollow structures

Zailei Zhang, Ji Chul Jung, Ning Yan*****

Department of Chemical and Biomolecular Engineering, National University of Singapore, 4 Engineering Drive 4, 117585 Singapore.

*To whom correspondence should be addressed. E-mail address: ning.yan@nus.edu.sg

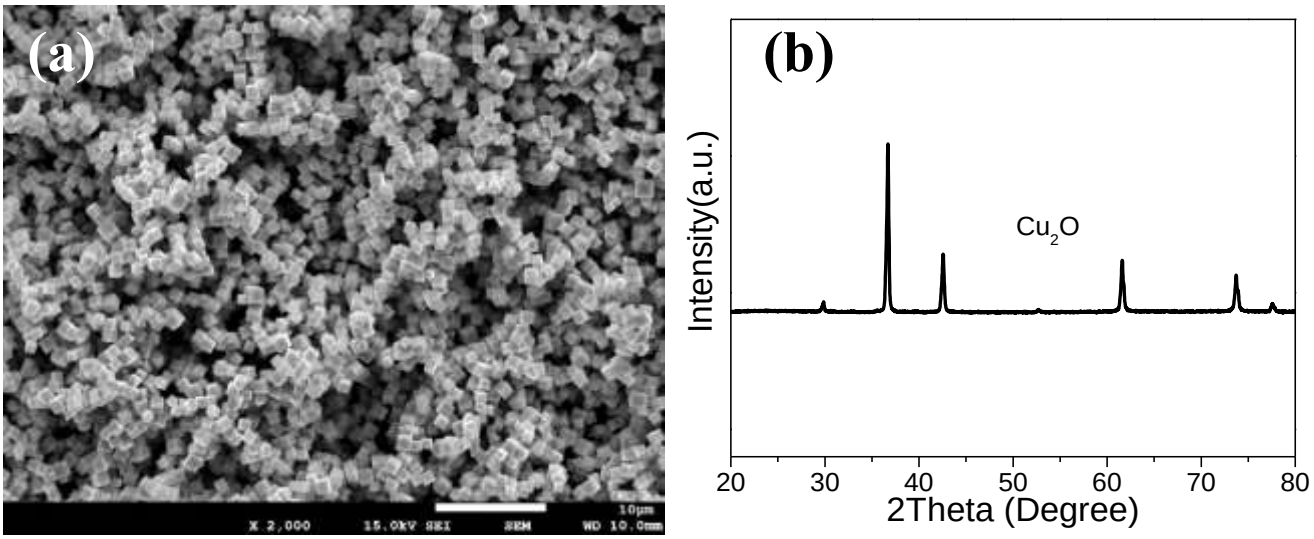

Fig. S1 SEM image (a) and XRD pattern (b) for Cu_2O cubes.

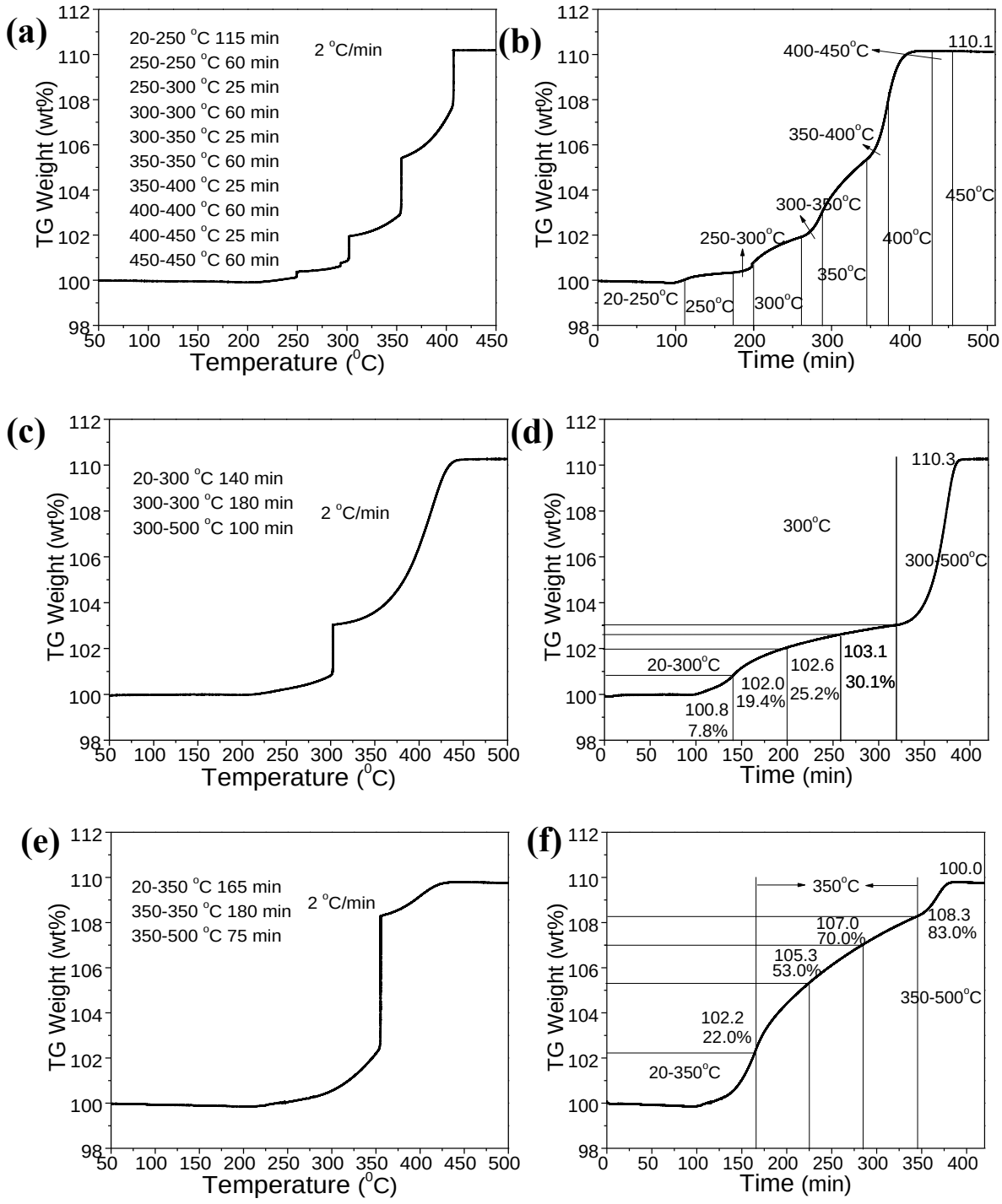

Fig. S2 TG curves for oxidation the Cu_2O cubes at different calcination temperature and time in air.

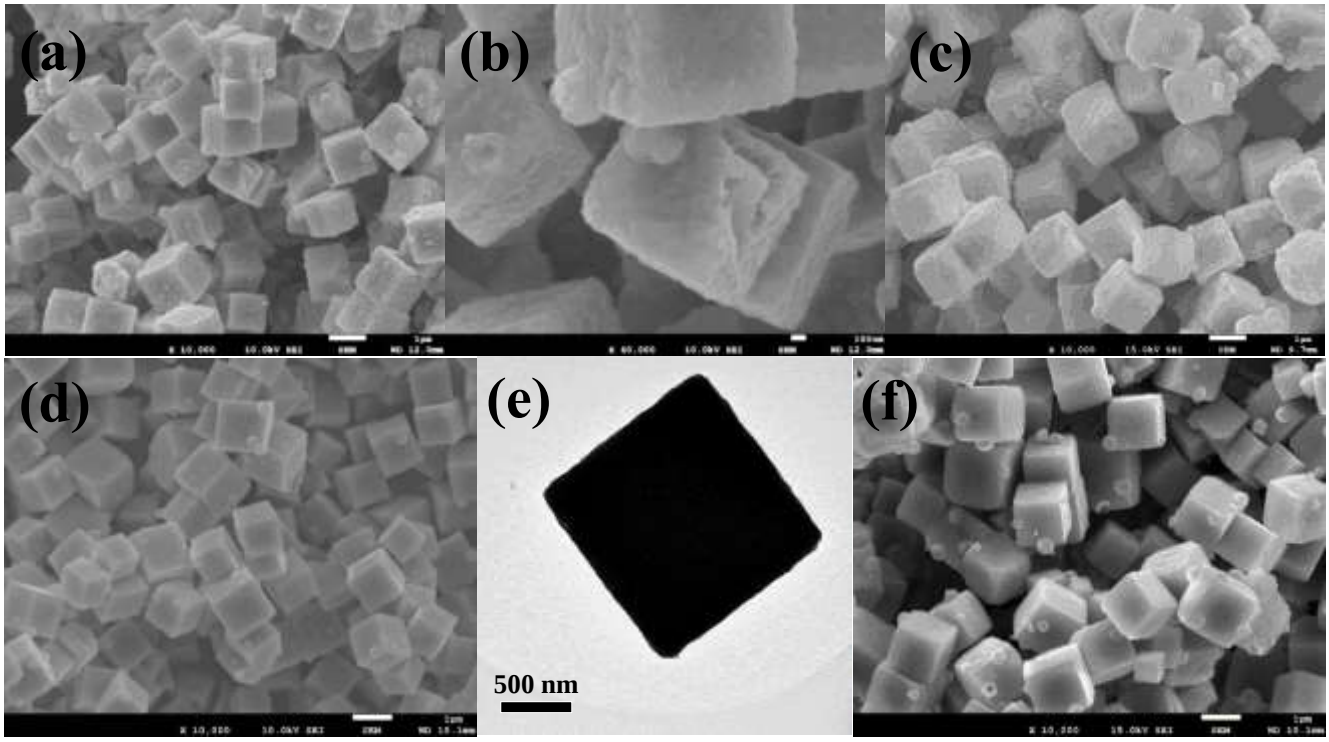

Fig. S3 SEM images of Cu_2O@CuO core-shell cubes after oxidation at 350 °C for 1 h (a and b), 350 °C for 2 h (c), 300 °C for 1 h (d), 300 °C for 2 h (f) in air, and TEM image of Cu_2O@CuO core-shell cubes after oxidation at 300 °C for 1 h (e).

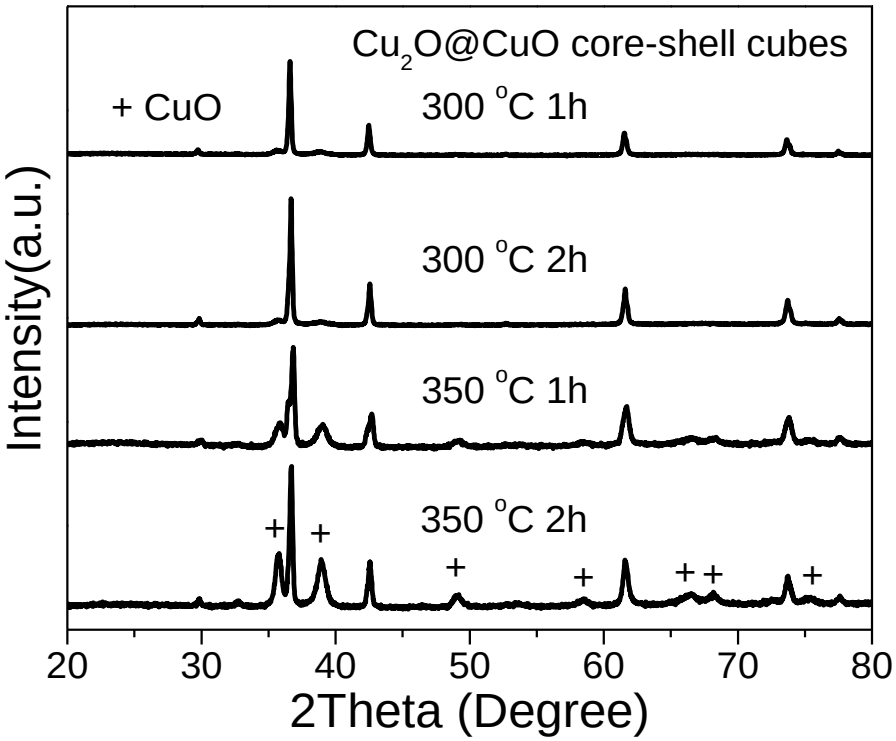

Fig. S4 XRD patterns for Cu_2O@CuO core-shell cubes after oxidation at 350 °C for 1 h, 350 °C for 2 h, 300 °C for 1 h, and 300 °C for 2 h.

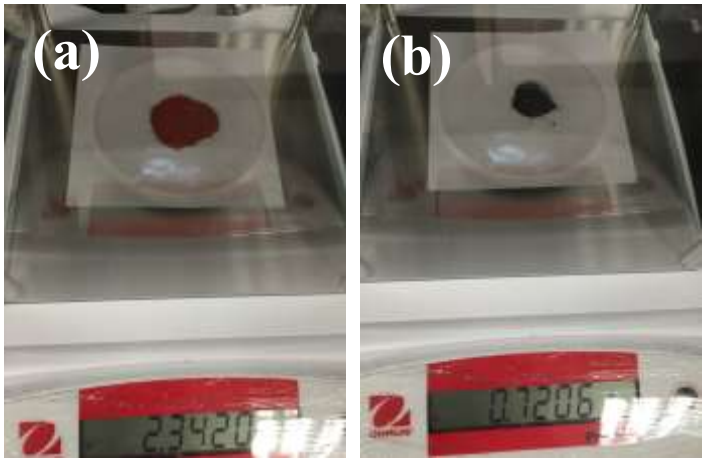

Fig. S5 Photographs of 2.3420 g Cu_2O cubes (a) and 0.7206 g CuO/Fe_2O_3 hollow cubes (b).

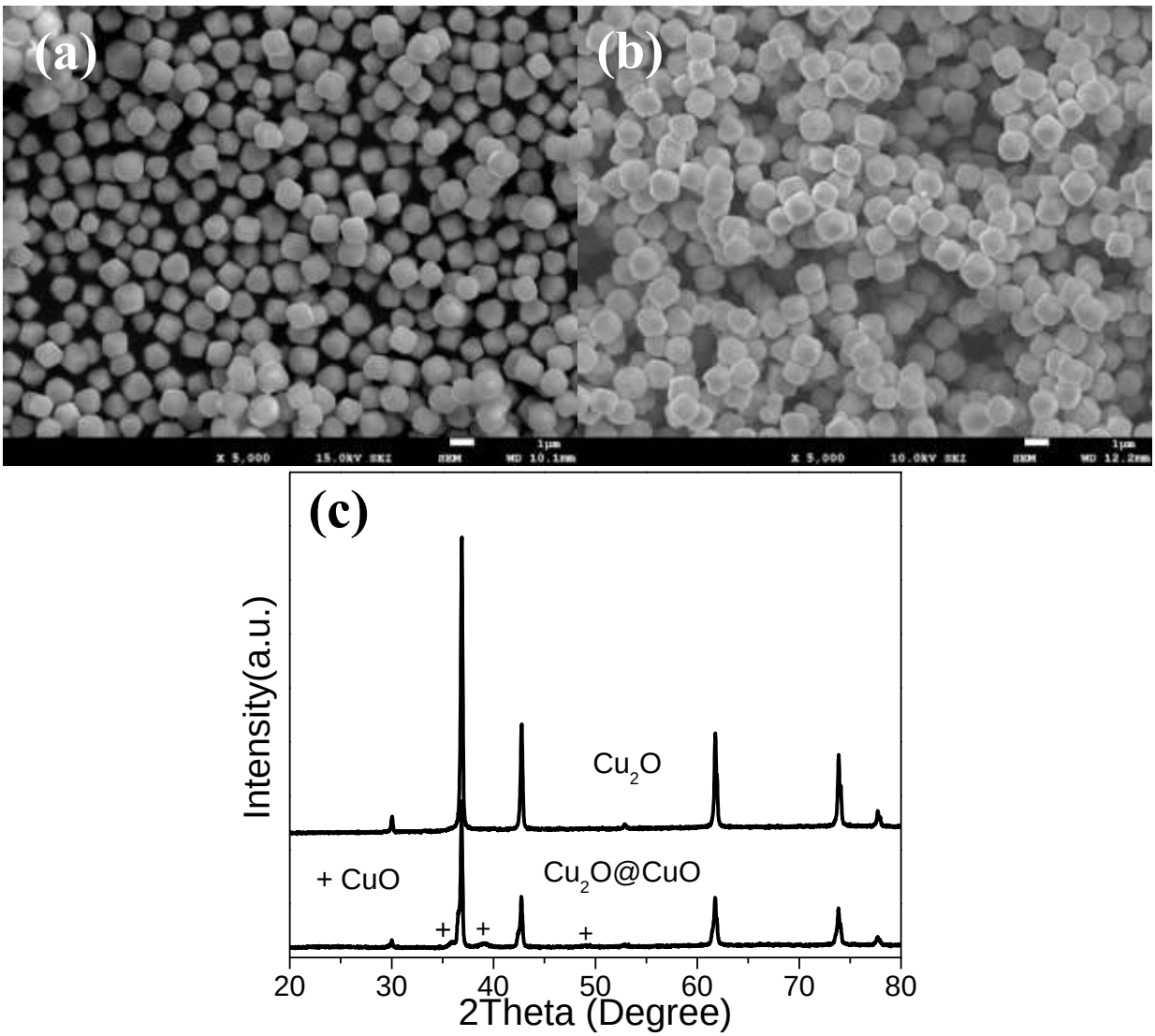

Fig. S6 SEM images of Cu_2O octahedrons (a), Cu_2O@CuO core-shell octahedrons after calcination at 300 °C for 1h in air (b), and XRD patterns for Cu_2O and Cu_2O@CuO core-shell octahedrons (c).

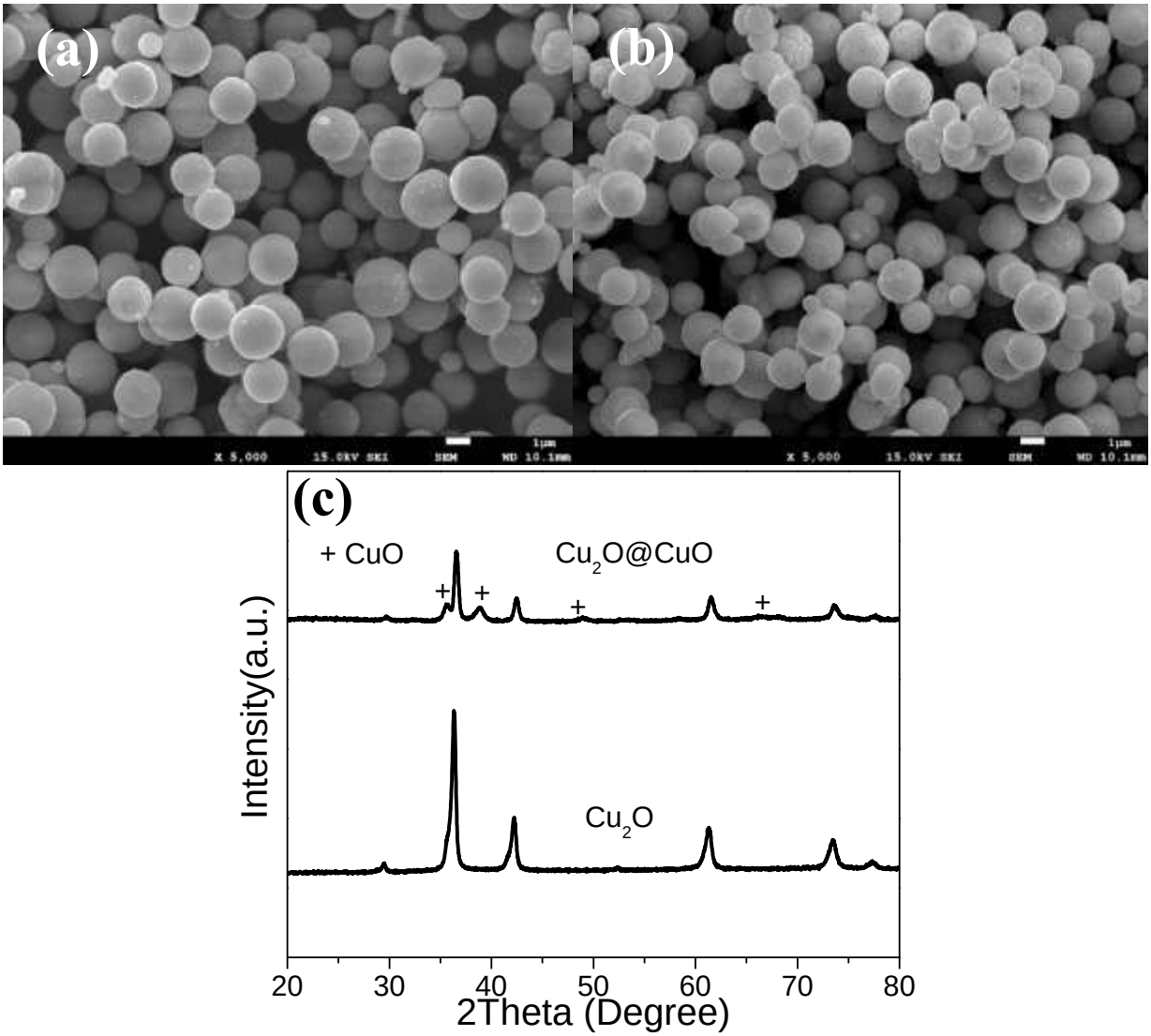

Fig. S7 SEM images of Cu_2O spheres (a), Cu_2O@CuO core-shell spheres after oxidation at 300 °C for 1 h in air (b), and XRD patterns for Cu_2O and Cu_2O@CuO core-shell spheres (c).

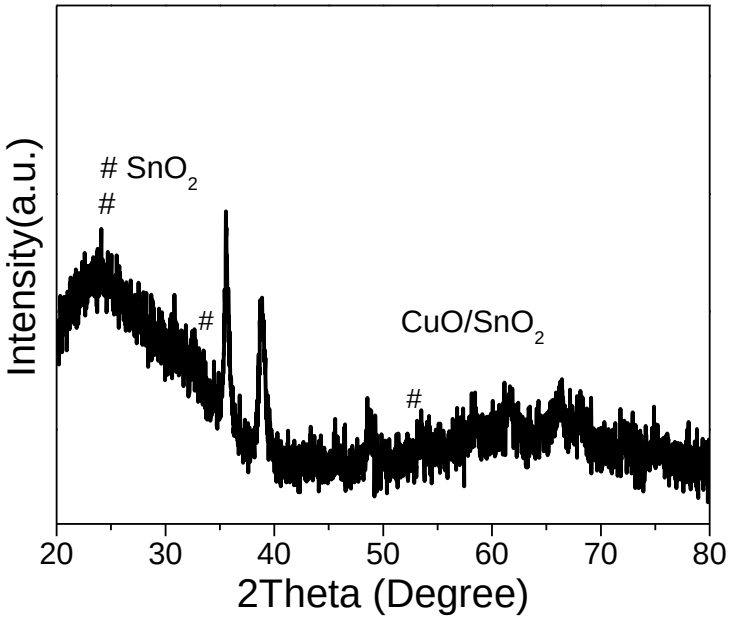

Fig. S8 XRD pattern for CuO/SnO_2 hollow cubes.

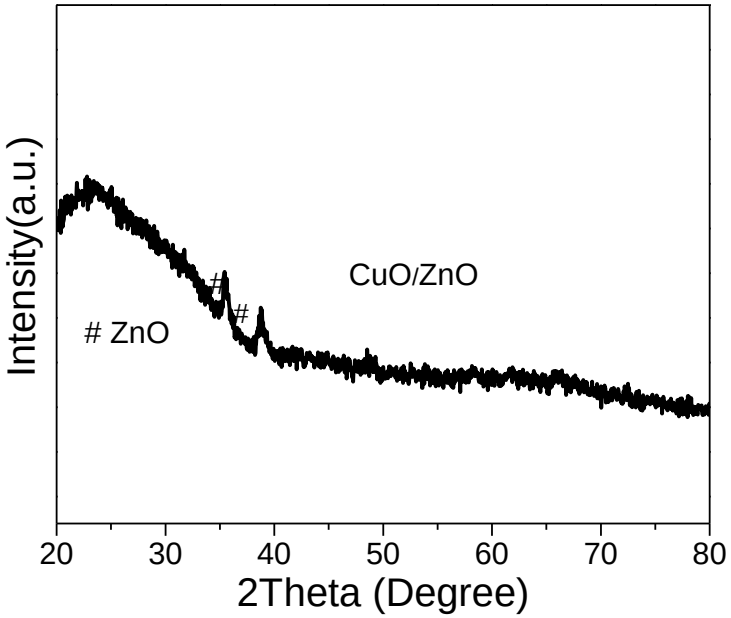

Fig. S9 XRD pattern for CuO/ZnO hollow cubes.

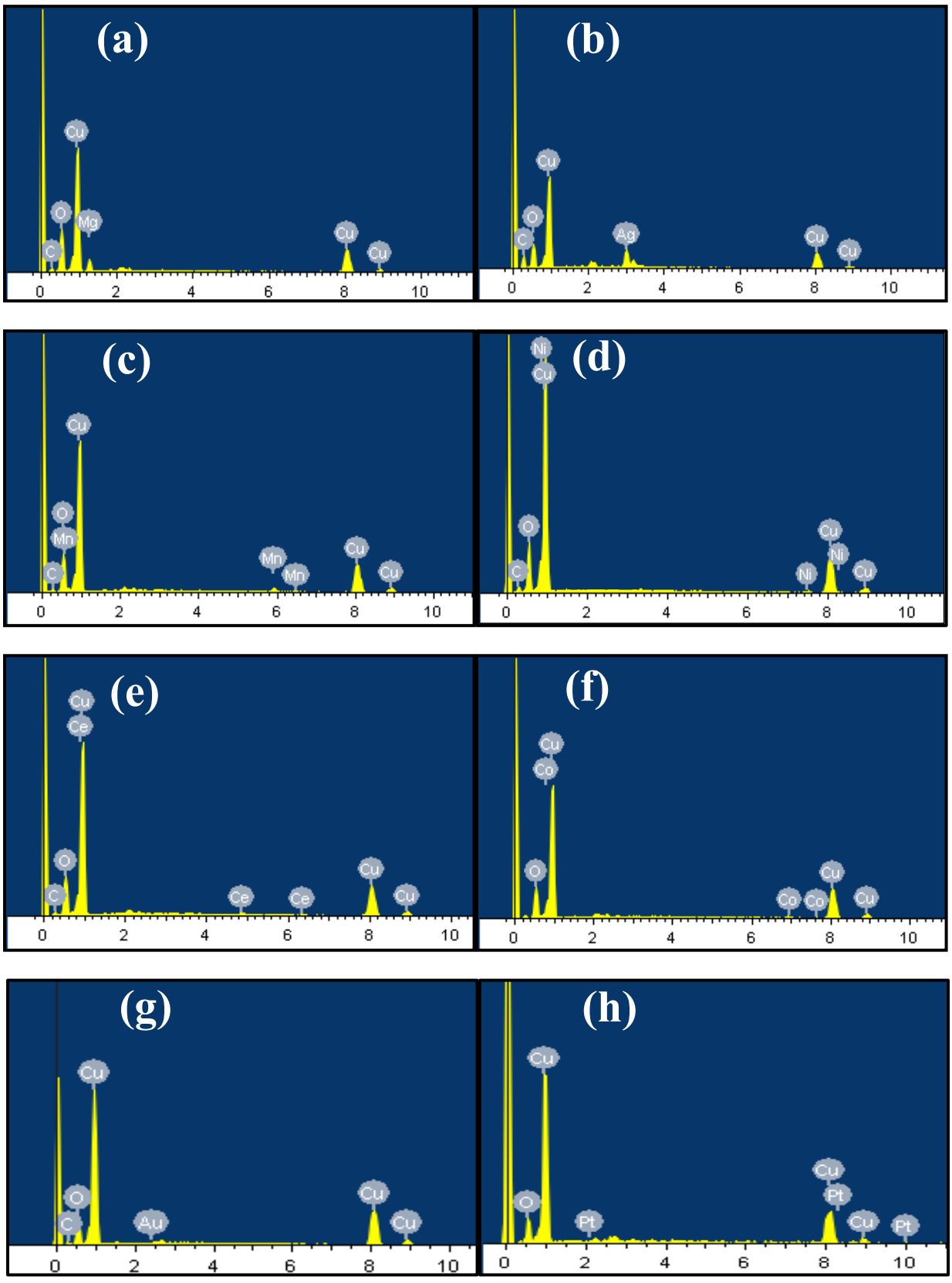

Fig. S10 EDX analyses of CuO/MgO (a), CuO/Ag_2O (b), CuO/Mn_2O_3 (c), CuO/NiO (d), CuO/CeO_2 (e), CuO/CoO (f), CuO/Au (g), and CuO/Pt (h) hollow cubes.

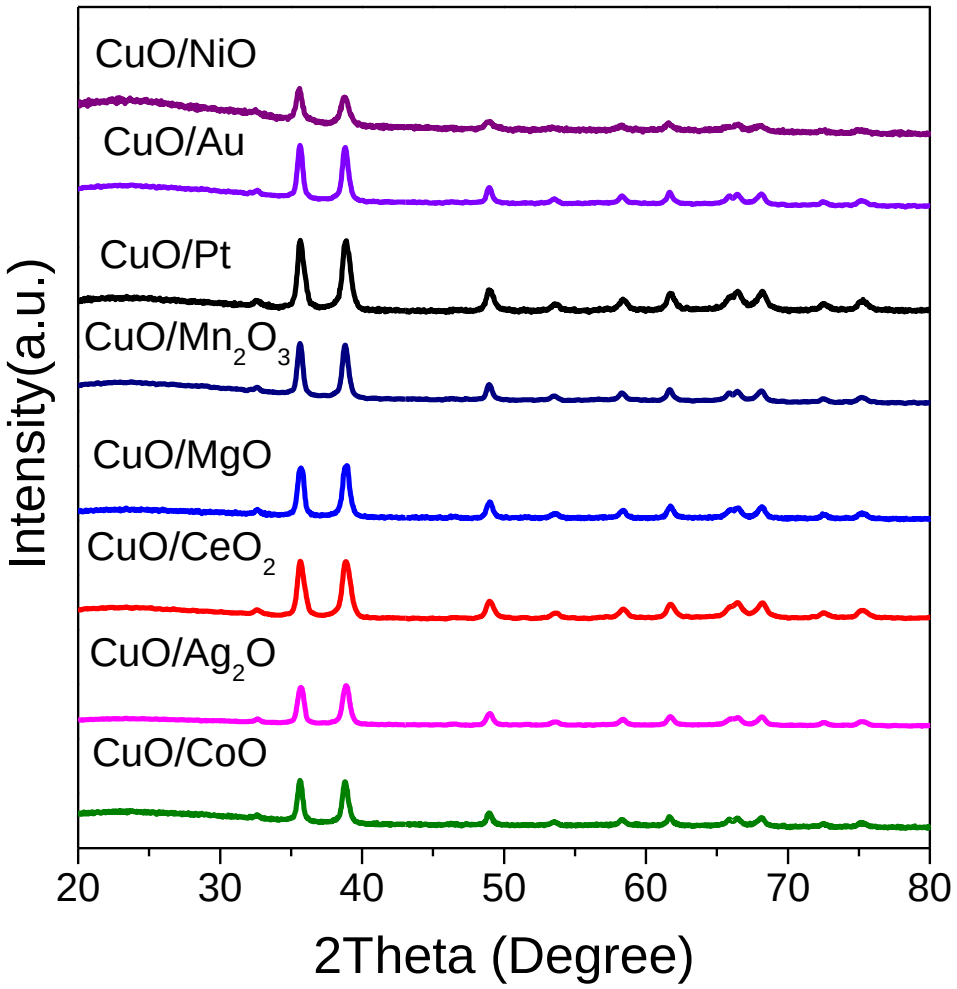

Fig. S11 XRD patterns for CuO/MgO, CuO/Ag_2O, CuO/Mn_2O_3, CuO/NiO, CuO/CeO_2, CuO/CoO, CuO/Au, and CuO/Pt hollow cubes.

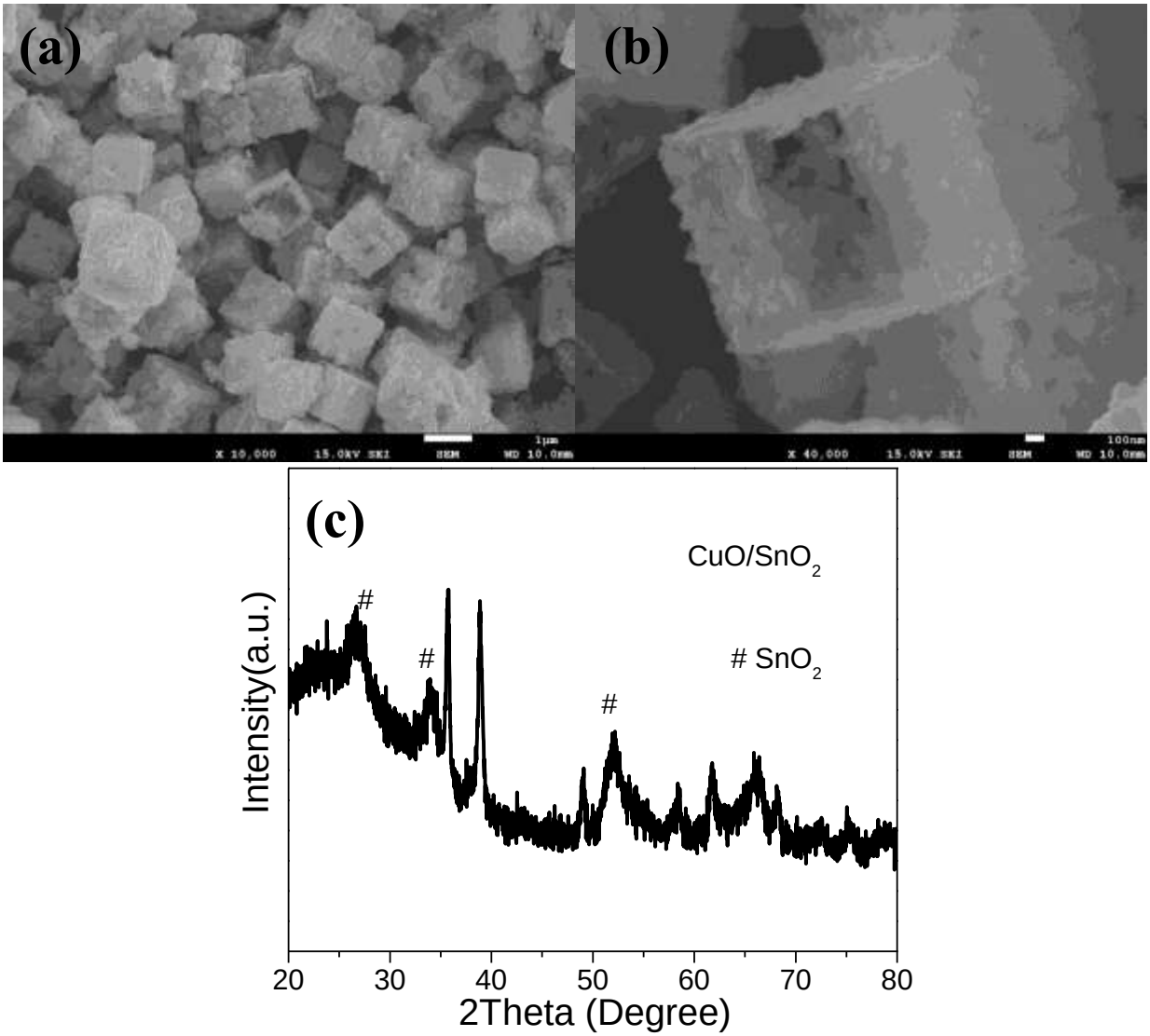

Fig. S12 SEM images (a and b) and XRD pattern (c) for CuO/SnO_2 hollow cubes after oxidation in air at 500 ^{o}C.

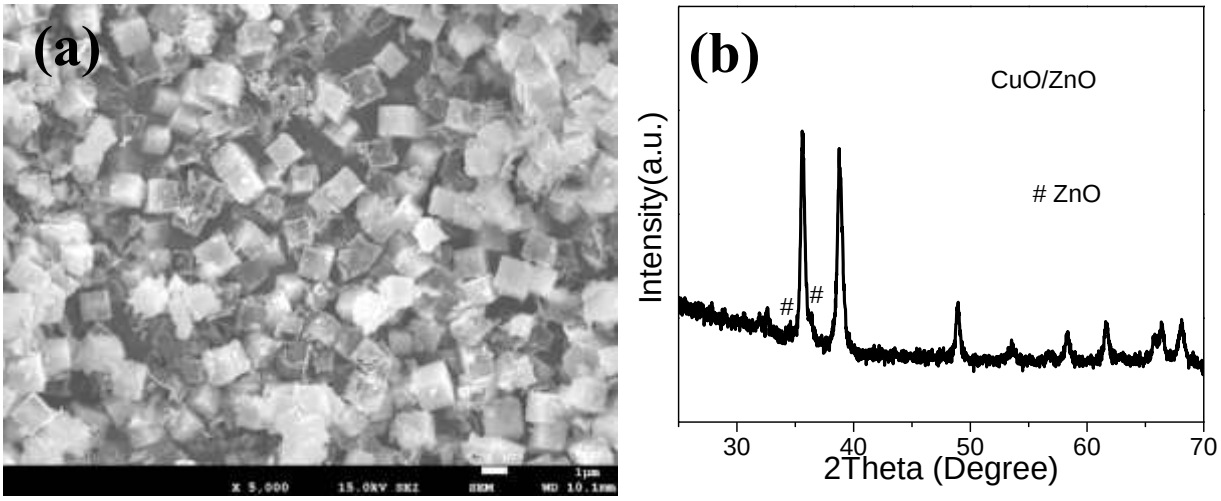

Fig. S13 SEM image (a) and XRD pattern (b) for CuO/ZnO hollow cubes after oxidation in air at 500 ^{o}C.

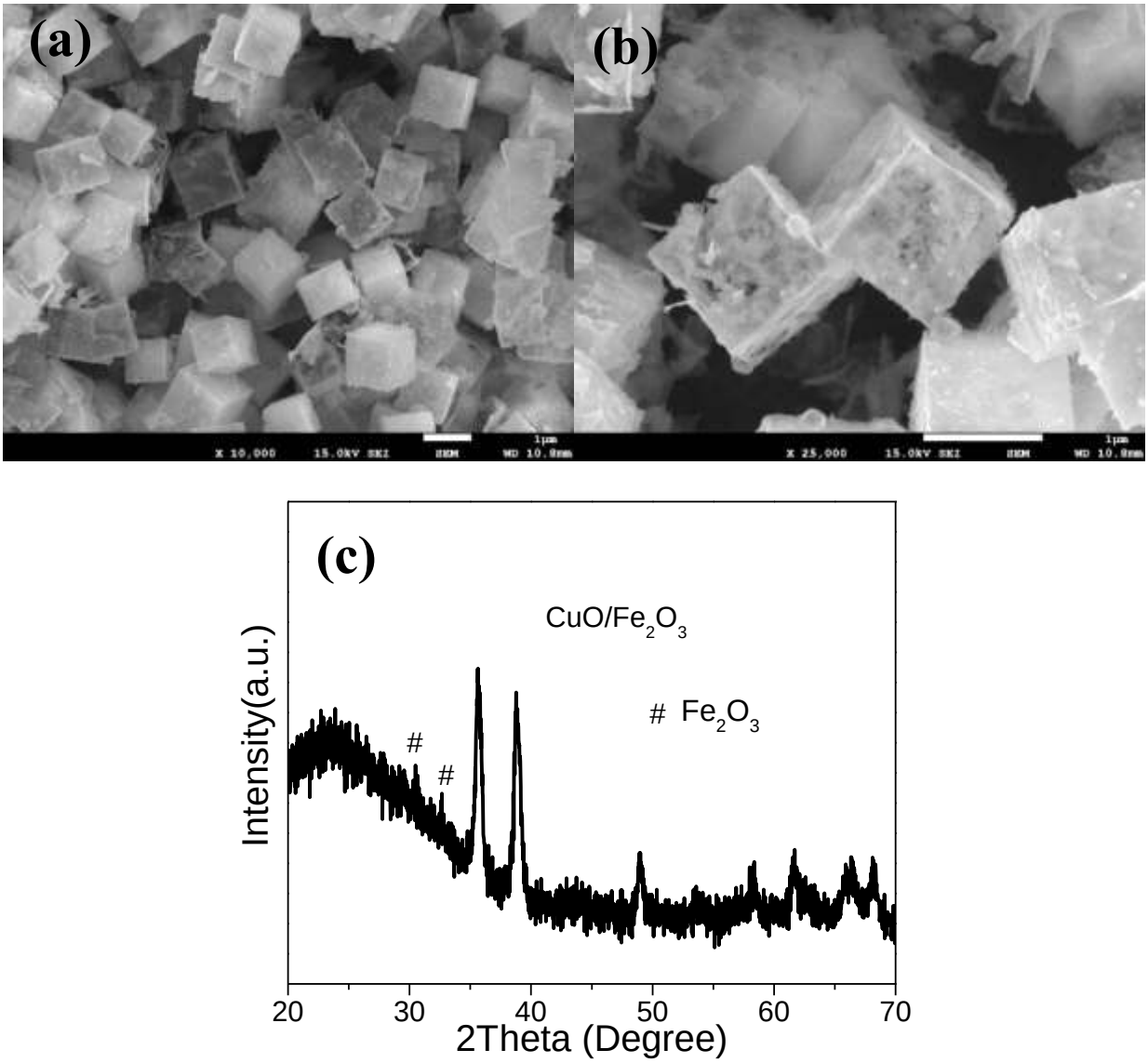

Fig. S14 SEM images (a and b) and XRD pattern (c) for CuO/Fe_2O_3 hollow cubes after oxidation in air at 500 ^{o}C.

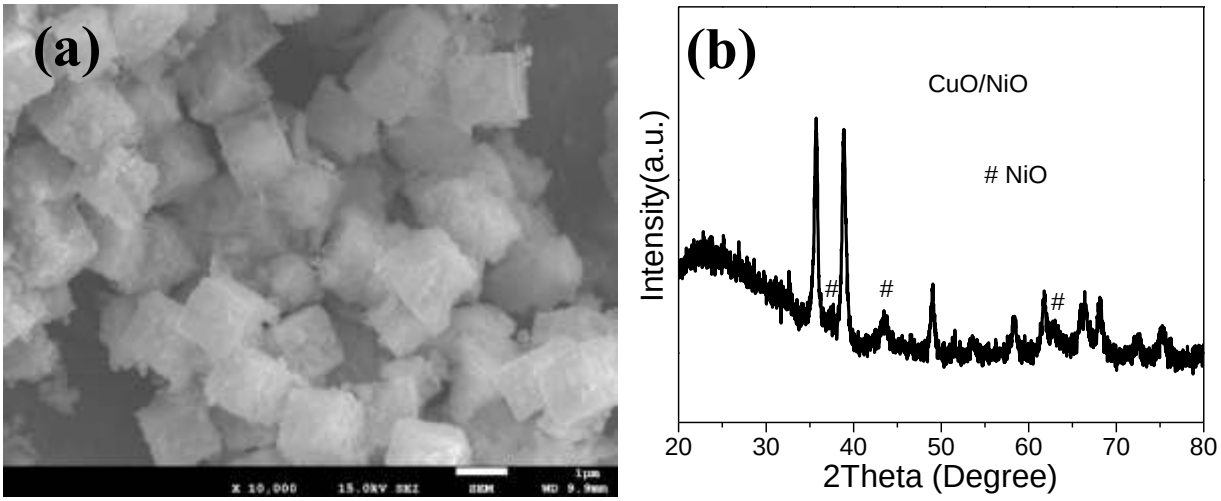

Fig. S15 SEM image (a) and XRD pattern (b) for CuO/NiO hollow cubes after oxidation in air at 500 ^{o}C.

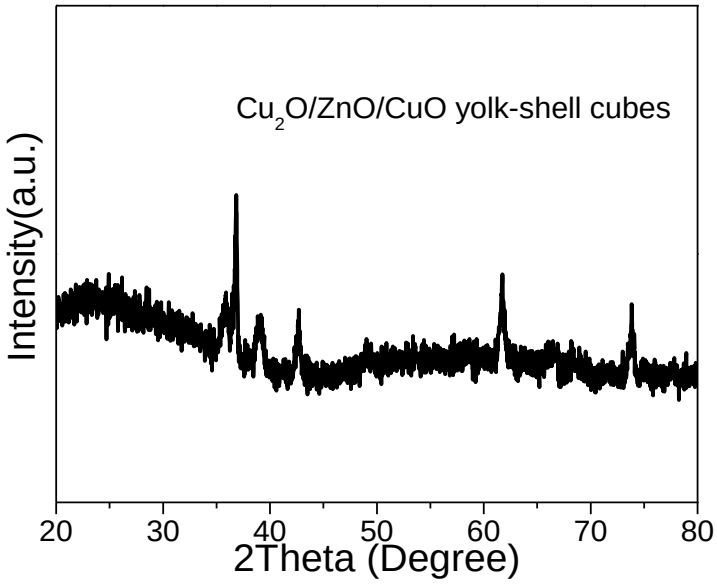

Fig. S16 XRD pattern for CuO/ZnO/Cu_2O yolk-shell cubes.

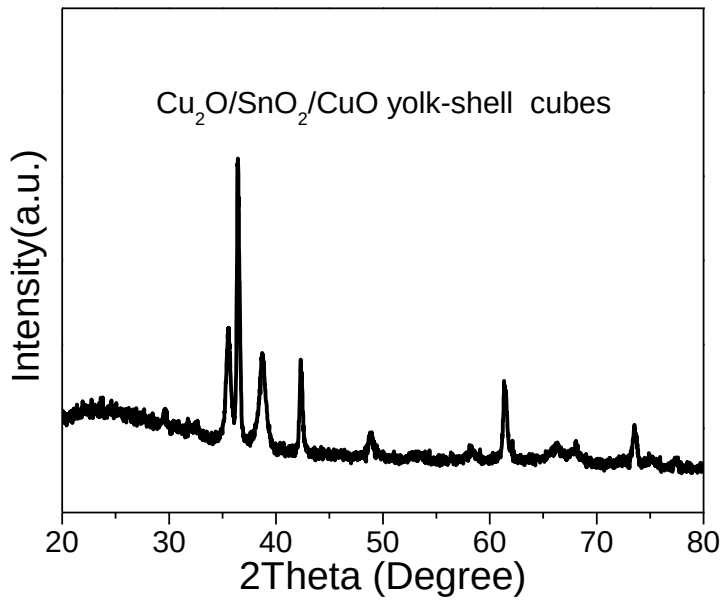

Fig. S17 XRD pattern for $CuO/SnO_2/Cu_2O$ yolk-shell cubes.

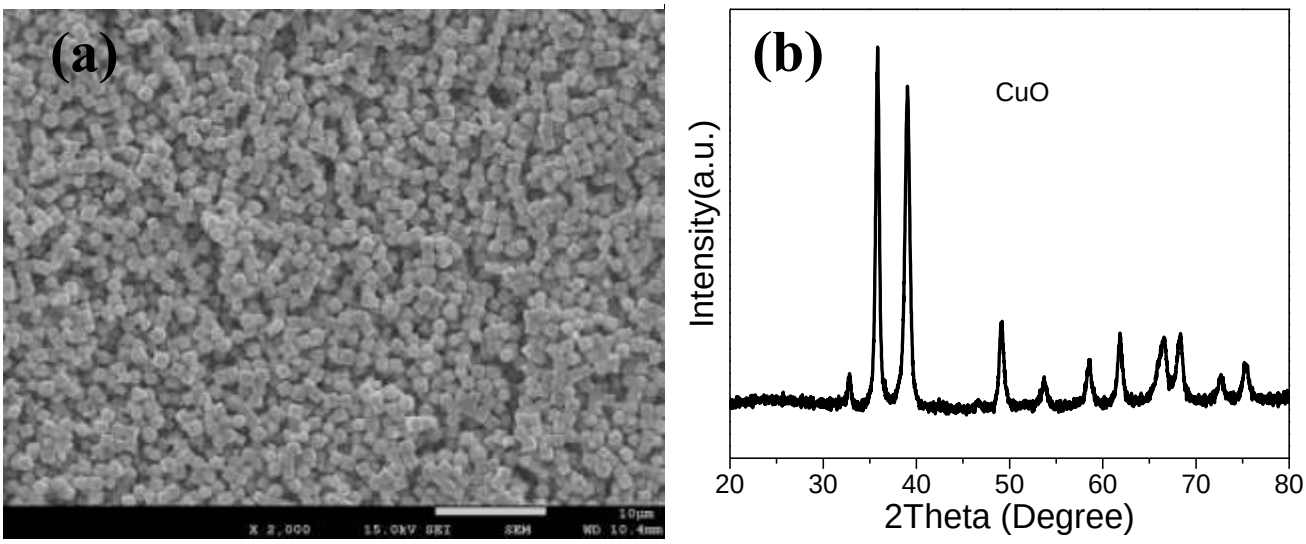

Fig. S18 SEM image (a) and XRD pattern (b) for CuO cubes after oxidation in air at 500 ^{o}C.

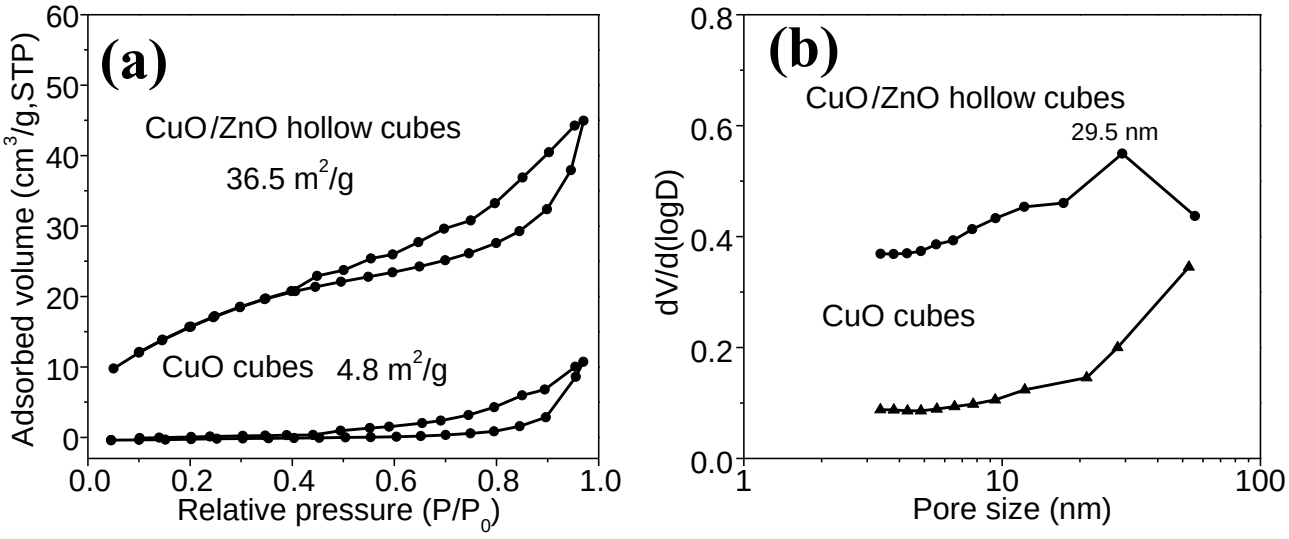

Fig. S19 N_2 adsorption-desorption isotherms (a) and their pore size distributions (b) of CuO cubes and CuO/ZnO hollow cubes (For clarity, the isotherm of CuO/ZnO hollow cubes was vertically shifted for 10 cm^3/g. Also, the pore size distribution of the samples was determined by applying the Barrett-Joyner-Halenda (BJH) method to the adsorption branch in the obtained N_2 adsorption-desorption isotherm).

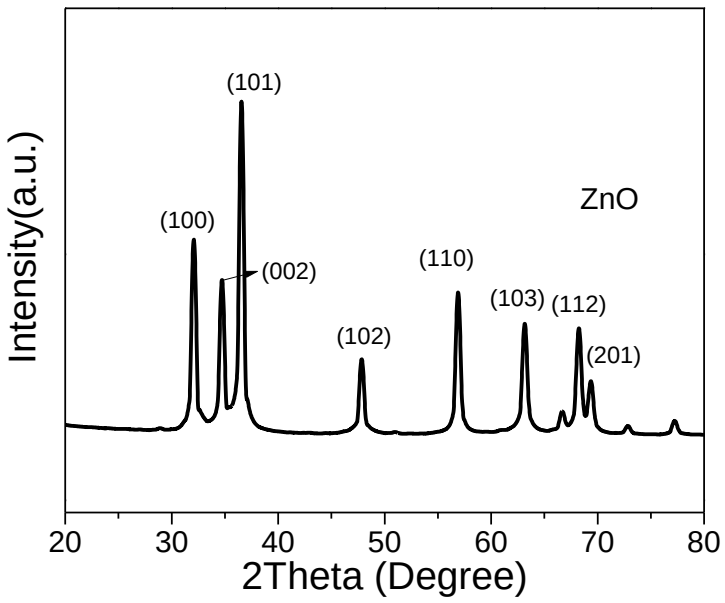

Fig. S20 XRD pattern of the prepared ZnO powder.

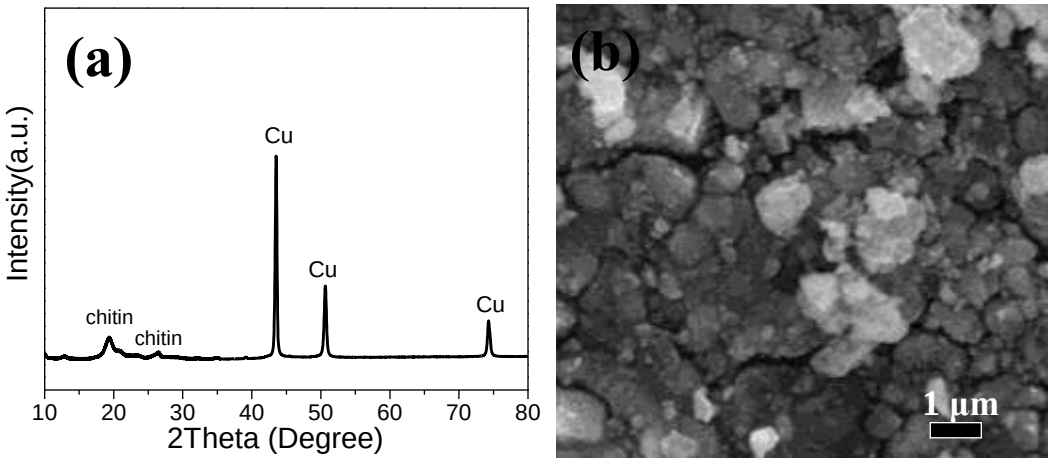

Fig. S21 XRD pattern (a) and SEM image (b) of the used CuO/ZnO hollow cubes after a catalytic chitin conversion at 300 °C for 4 h.

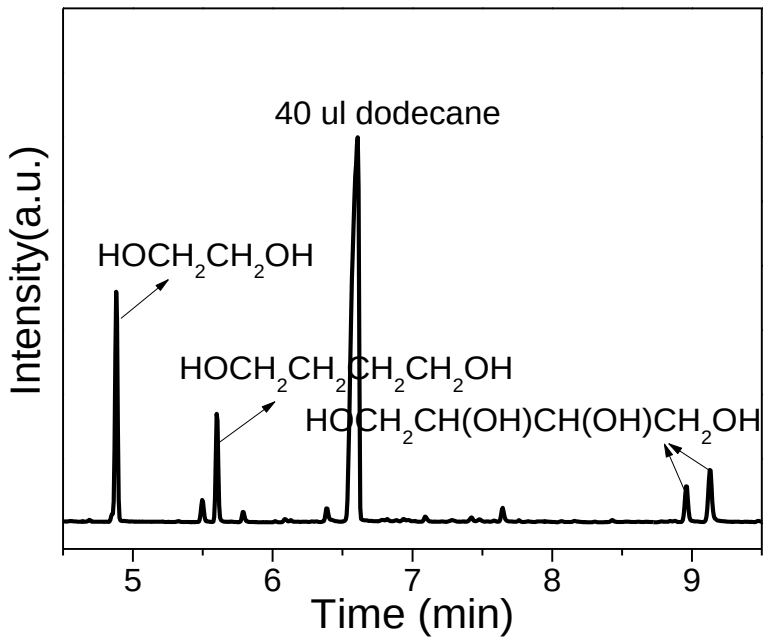

Fig. S22 Typical GC-MS chromatogram after TMS derivatization. For simplification, the corresponding molecular formulas are presented in the Figure instead of the TMS derivate molecules. After the catalytic reaction, the dodecane is added as a reference.

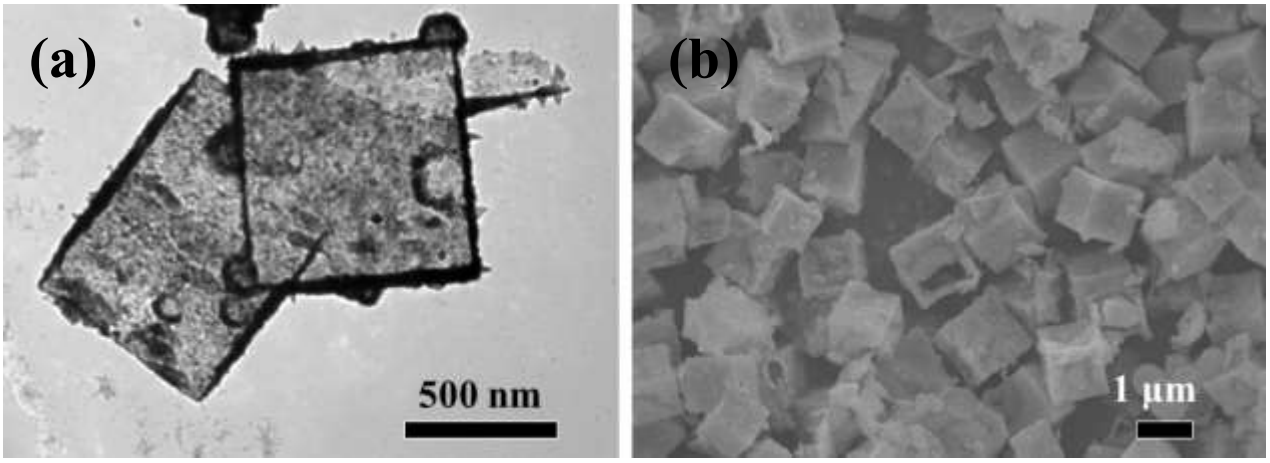

Fig. S23 TEM image (a) and SEM image (b) of CuO/ZnO double-shell hollow cubes after four cycle tests for benzyl alcohol oxidation.

Table S1. Effect of reaction temperature on the conversion of chitin over CuO, CuO/ZnO hollow cubes, and CuO+ZnO catalysts.

Conversion	240°C	260°C	280°C	300°C
CuO	20.6	25.1	30.5	36.2
CuO/ZnO	24.3	30.2	42.5	50.3
CuO+ZnO[a]				43.6
Without catalyst	/	/	/	12.0
CuO/ZnO in 5 ml toluene	/	/	/	20.1

Reaction conditions: 5 ml methanol, 100 mg chitin, 50 mg CuO, CuO/ZnO, CuO+ZnO catalysts, 400 rpm, reaction time 4 h. After the catalytic reaction, the dodecane was added as an internal standard.

[a]CuO+ZnO catalyst was prepared by a physical mixing of 49 mg CuO solid cubes and 11 mg ZnO power, which was obtained via calcination of zinc nitrate ($Zn(NO_3)_2$) at 500 °C for 2 h under static air condition. For the confirmation of successful formation, XRD patterns of the prepared ZnO powder was also presented in Fig. S20.

Table S2. The conversion of benzyl alcohol and selectivity of benzaldehyde (1) and benzoic acid (2) over CuO or without CuO catalysts in air and pure O_2 condition.

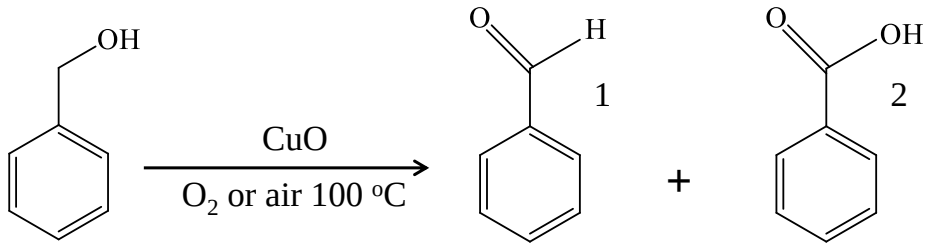

Samples	Conversion/%	Selectivity of 1/%	Selectivity of 2/%
Air 100^{o}C (CuO)	0.3	~100	~0
Air 100^{o}C without catalyst	~0	~0	~0
100^{o}C 0.5 MPa O_2 (CuO)	0.5	~100	~0
100^{o}C 0.5 MPa O_2 without catalyst	~0	~0	~0

Reaction conditions: 0.58 mmol benzyl alcohol, 3.0 ml toluene, 500 rpm, 20 mg CuO catalyst, reaction time 12 h. After the catalytic reaction, the dodecane is added as a reference.

Table S3. The conversion of benzyl alcohol and selectivity of benzaldehyde (1) and benzoic acid (2) over CuO, CuO/Ag_2O, CuO/Pt and CuO/Au catalysts in pure O_2 condition.

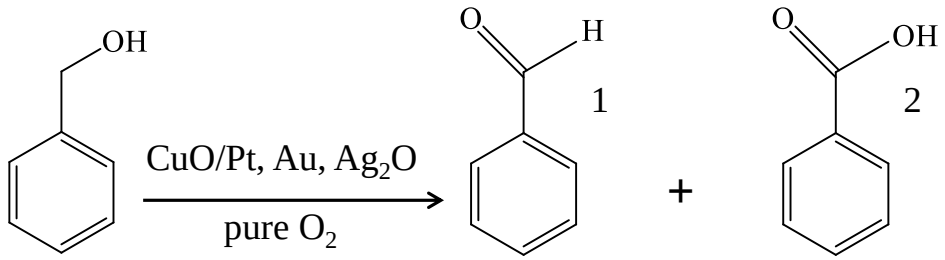

Samples	Conversion/%	Selectivity of 1/%	Selectivity of 2/%	TOF (h^{-1})[a]
CuO	~0	~0	~0	
CuO/Au	43.6	~100	~0	2.0
CuO/Pt	61.2	~100	~0	3.5
CuO/Ag_2O	1.0	~100	~0	

Reaction conditions: 0.58 mmol benzyl alcohol, 3.0 ml toluene, 500 rpm, 20 mg catalyst, 0.5 MPa O_2, reaction time: 18 h, reaction temperature: 50 ^oC, benzyl alcohol : Pt = 102 : 1 (molar), benzyl alcohol : Au = 84 : 1 (molar). After catalytic reaction, dodecane was added as a reference.

[a] TOF was calculated on the basis of total loading of Pt and Au.